

Coupled substitution of NiO and TiO₂ in haematite

B.-H. PARK, H. SUITO

Institute for Advanced Materials Processing, Tohoku University, Katahira, Aoba-ku, Sendai 980, Japan

The partitionings of NiO and of NiO and TiO₂ between haematite and Na₂O·2B₂O₃ melts were studied by the flux growth method as a function of solute concentration. The substitution mechanisms of NiO and/or TiO₂ in α -Fe₂O₃ lattice are discussed based on the results of concentration dependence of the distribution coefficients. The substitution of the Ni²⁺ ion on Fe³⁺ sites was accompanied by the charge compensating oxygen ion vacancies, while the coupled substitution of Ni²⁺ and Ti⁴⁺ ions on Fe³⁺ sites was accompanied by the formation of Fe²⁺ ions, confirmed by chemical analysis.

1. Introduction

It is well known that the impurities and size distribution of α -Fe₂O₃, which is the main raw material for the ferrite products, have a significant effect on its magnetic properties. Therefore, thermodynamic studies on trace (or minor) elements in α -Fe₂O₃ are indispensable in clarifying the impurity behaviour. A series of experiments on the distribution coefficients between α -Fe₂O₃ crystals and Na₂O–B₂O₃ flux was carried out; the manganese, Al₂O₃, and TiO₂ partitions have been reported elsewhere [1–3].

The purpose of this investigation was to elucidate the mechanism of the coupled substitution of NiO and TiO₂ in an α -Fe₂O₃ lattice. For the measurement of the distribution coefficients of NiO and/or TiO₂ between α -Fe₂O₃ crystal and Na₂O·2B₂O₃ flux, the method of crystal growth by Ostwald ripening was used in the present work.

2. Experimental procedure

2.1. Methods

The materials used in the present work were α -Fe₂O₃ (Rare Metallic, Fe₂O₃ > 99.99 wt %), and reagent grades of Na₂B₄O₇, NiO, and TiO₂. The average size of α -Fe₂O₃ crystals determined by scanning electron microscope (SEM) observation was 0.1 μ m. An excess amount of α -Fe₂O₃ powder, which was about 1.5 times greater than the solubility [1], was mixed with the Na₂O·2B₂O₃ flux. Samples (20–30 g) in a platinum crucible were placed in the constant-temperature zone of a vertical SiC resistance furnace and stirred with a platinum stirrer (10 rad s⁻¹) to make the liquid composition homogeneous. The experiments were conducted under a dry air atmosphere at temperatures ranging from 800–1100 °C in the experiments of NiO partitioning and at 1000 °C in those of the coupled substitution of NiO and TiO₂. In most experiments, the solute in α -Fe₂O₃ crystals was taken up from the solution side.

After holding a sample at temperature for 6–12 h, the sample was quenched into water. No α -Fe₂O₃ crystal was precipitated during quenching. The content of each element in the solid and liquid phases of the sample was measured by wet chemical analysis. More detailed descriptions are given in previous papers [1, 2].

2.2. Analysis

The sample was washed in boiling HCl (2 + 50) solution with a volume of 100 ml per 1 g sample, for 30 min, to dissolve the flux. Thereafter, the aqueous solution was separated from the crystals by pressurized filtration, using a 0.1 μ m membrane filter. H₂SO₄ (1 + 35) was used with samples containing TiO₂. The flux compositions were determined by analysing the filtrate. α -Fe₂O₃ crystals were dissolved in 10 ml hot HCl (1 + 1) per 0.2 g crystals.

The Fe²⁺ ion content in α -Fe₂O₃ crystals was determined by potassium dichromate titration, dissolving crystals with HCl (1 + 1) under a dry CO₂ atmosphere. Atomic absorption spectrometry was used for the analysis of sodium, and induced coupled plasma (ICP) emission spectrometry (SEIKO SPS-1200A) for the analysis of the other elements.

The content of each element in the α -Fe₂O₃ crystal as well as in the flux was analysed by electron probe micro-analysis (EPMA, Hidachi X650S) at an accelerating voltage of 15 kV for all elements. The results were in good agreement with those obtained by chemical analysis. The homogeneity of nickel and titanium in crystal grains was confirmed by line analysis of EPMA.

3. Results and discussion

3.1. Crystal growth by Ostwald ripening

The initial α -Fe₂O₃ crystals with an average size of 0.1 μ m in saturated solution were found to grow to

a size of 10–20 μm over a period of 6–12 h. The observed coarsening of the crystals was confirmed to be due to the Ostwald ripening mechanism in which the driving force is the reduction of total interfacial energy of the larger crystals. The details of this mechanism are discussed elsewhere [1, 2].

The partitioning of minor elements occurs under equilibrium conditions during Ostwald ripening, due to the low degree of supersaturation with respect to crystal growth. This was confirmed by examining the homogeneity and time dependence of the solute content in the crystal grain; that is, in the present work, the concentration of solute within a crystal was homogeneous and constant with time. Furthermore, in previous work [1, 2] the equilibrium partitioning was confirmed by examining the effect of initial grain size on the distribution coefficient, and the reversal experiment in which solute element was dissolved from crystal into flux, was carried out. These previous experimental findings lead to the conclusion that the equilibrium distribution coefficients can be obtained using the flux growth method. The contents of Na_2O and B_2O_3 in $\alpha\text{-Fe}_2\text{O}_3$ were analysed to be 10–25 and 10–30 wt p.p.m., respectively.

3.2. Substitution of NiO by defect formation

The distribution coefficient of NiO between solid and liquid phases is defined as

$$k_{\text{NiO}} = x_{\text{NiO}}^s / x_{\text{NiO}}^l \quad (1)$$

where x_{NiO}^s and x_{NiO}^l represent the mole per cent of NiO in solid and liquid phases, respectively.

The relationships between the distribution coefficient of NiO and the content of NiO in the $\text{Na}_2\text{O} \cdot 2\text{B}_2\text{O}_3$ flux expressed in mole per cent, are plotted as a function of temperature in Fig. 1. It can be seen that the values for the distribution coefficient of NiO decrease with increasing content of NiO in the flux.

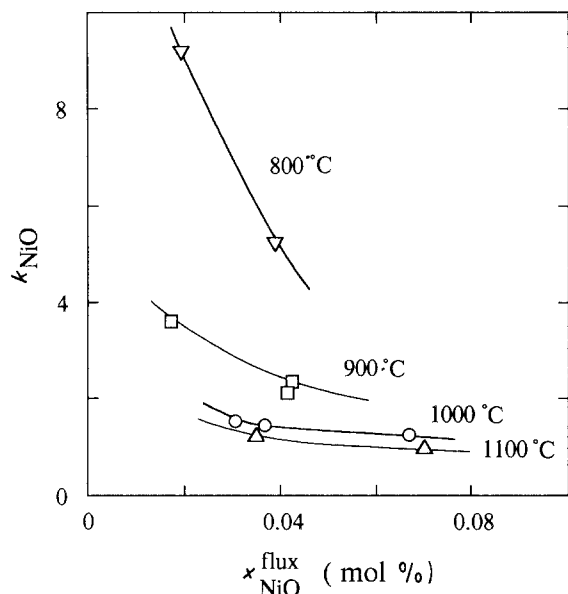
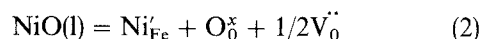


Figure 1 Distribution coefficient of NiO plotted against the NiO content in the flux as a function of temperature.

When an ion having a different valence enters the substitutional site at compositions of greater than thermal defect concentration, lattice defects are produced for charge neutrality reasons. This results in a decreased distribution coefficient [3–5]. Although the distribution coefficient also depends on a solution interaction factor, it is likely in the present experimental conditions that it will be much more sensitive to changes in solid phase.

Incorporation of NiO into $\alpha\text{-Fe}_2\text{O}_3$ by the substitution of the Ni^{2+} ion on Fe^{3+} sites leads to charge compensating oxygen ion vacancies according to the following equation using the Kröger and Vink notation [7]



The equilibrium constant, K_2 , for the reaction given by Equation 2 can be expressed by

$$K_2 = [\text{Ni}_{\text{Fe}}^i][\text{V}_0^{\cdot\cdot}]^{1/2} f(\gamma) / x_{\text{NiO}}^l \quad (3)$$

where $[i]$ and x_i denote the molar concentration of component i and $f(\gamma)$ is the respective activity coefficient term. The activity of O_0^x remains essentially constant and can be taken as unity.

Salmon [8] has reported that Fe_2O_3 is oxygen deficient and for Fe_2O_3 in equilibrium with Fe_3O_4 , the value of x in $\text{Fe}_2\text{O}_{3-x}$ ranges from 0.0015 at 1000 °C to 0.011 at 1450 °C. Thus, provided that the concentration of thermal oxygen vacancy is negligible, we can write

$$[\text{V}_0^{\cdot\cdot}] = 1/2[\text{Ni}_{\text{Fe}}^i] \quad (4)$$

By substituting Equation 4 into Equation 3 and expressing $[\text{Ni}_{\text{Fe}}^i]$ by x_{NiO}^s , we have

$$x_{\text{NiO}}^s = C_1 \{K_2 f(\gamma)\}^{2/3} (x_{\text{NiO}}^l)^{2/3} \quad (5)$$

where C_1 is the constant under the present experimental conditions. If a dilute solution behaviour (Henry's law) is valid with respect to NiO in both phases, it can be expected that x_{NiO}^s is proportional to

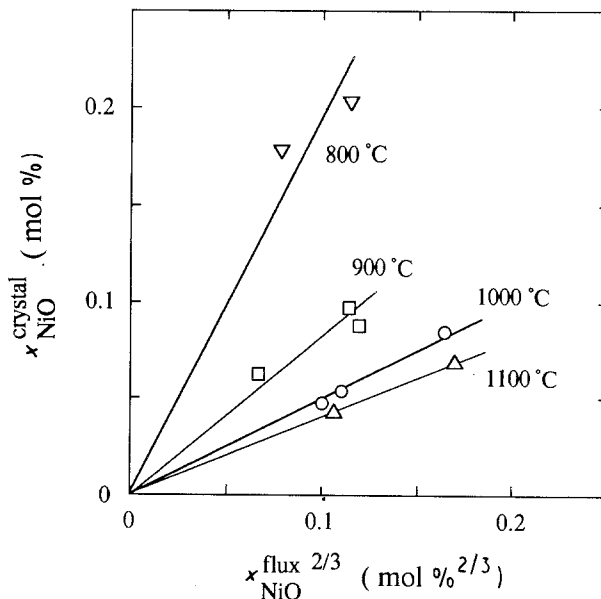


Figure 2 NiO content in the crystal plotted against the two-thirds power of NiO content in the flux.

$x_{\text{NiO}}^{\text{L}}$ to the power of 2/3. This relationship is shown in Fig. 2, demonstrating a good linearity at respective temperatures.

The importance of thermal defects in the very low concentration region has been confirmed experimentally by Harrison and Wood [9] who studied the partitioning of samarium and thulium between garnets and melts. They found that the distribution coefficient becomes constant at very low concentrations of rare-earth metals. Wagner [10] also discussed the decisive role of lattice defects on the distribution of SrCl_2 between solid and liquid KCl.

3.3. Coupled substitution of NiO and TiO_2

The charge-compensating substitutions are termed coupled diadochy [11] or compensatory solid solution [12]. "Coupled substitution" is designated by Nassau [5] who studied the distribution of various rare-earths in the Czochralski growth of calcium tungstate crystals from the melt. In this paper, the designation "coupled substitution" is used.

The coupled substitution of NiO and TiO_2 in $\alpha\text{-Fe}_2\text{O}_3$ is discussed in this section based on results obtained in the NiO and TiO_2 partitioning experiments.

The values for k_{TiO_2} are plotted against the NiO content in flux, as a function of TiO_2 content in flux in Fig. 3, in which the results at $x_{\text{NiO}}^{\text{flux}} = 0$ correspond to those obtained at 1000 °C in the previous experiment [3] of TiO_2 partitioning. It can be seen that the values for k_{TiO_2} increase with an increase of NiO content in the flux at constant TiO_2 content in the flux.

In order to explain the mechanism for coupled substitution, the content of Fe^{2+} ions in $\alpha\text{-Fe}_2\text{O}_3$ was determined by chemical analysis. The sum of the FeO

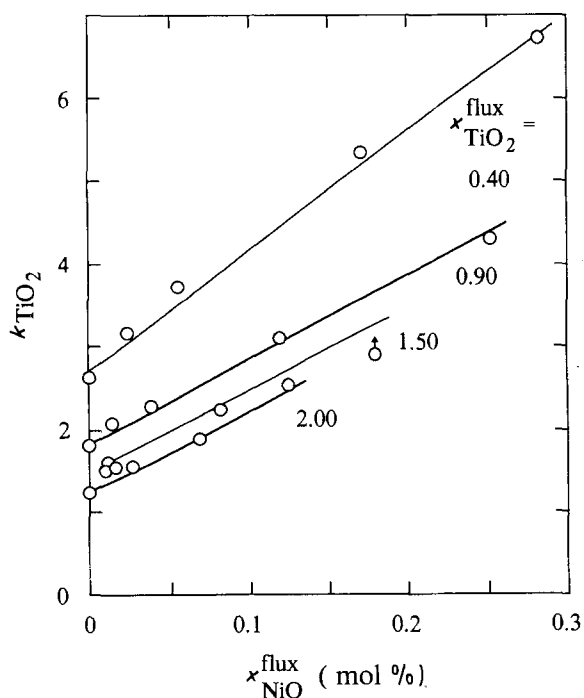


Figure 3 Effect of NiO content in the flux on k_{TiO_2} as a function of TiO_2 content in the flux at 1000 °C.

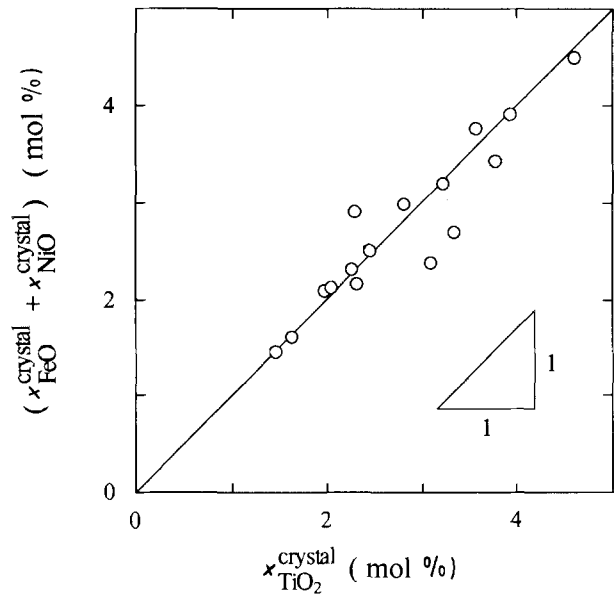


Figure 4 Relationship between the sum of FeO and NiO contents and the TiO_2 content in the crystal at 1000 °C.

and NiO contents in $\alpha\text{-Fe}_2\text{O}_3$ is plotted against the TiO_2 content in the crystal in Fig. 4, in which a reasonable linearity was obtained. This implies that 2 mol Fe^{3+} ion substitutes for x mol Ni^{2+} ion, $(1-x)$ mol Fe^{2+} ion, and 1 mol Ti^{4+} ion.

The values for k_{NiO} are plotted against the TiO_2 content in the flux as a function of NiO content in the flux in Fig. 5. The results at $x_{\text{TiO}_2}^{\text{flux}} = 0$ correspond to those obtained at 1000 °C in NiO partitioning experiments in the previous section. This marked increase of k_{NiO} seems to indicate that the coupled substitution unaccompanied by formation of a lattice defect in $\alpha\text{-Fe}_2\text{O}_3$ via the charge-balanced mechanism requires

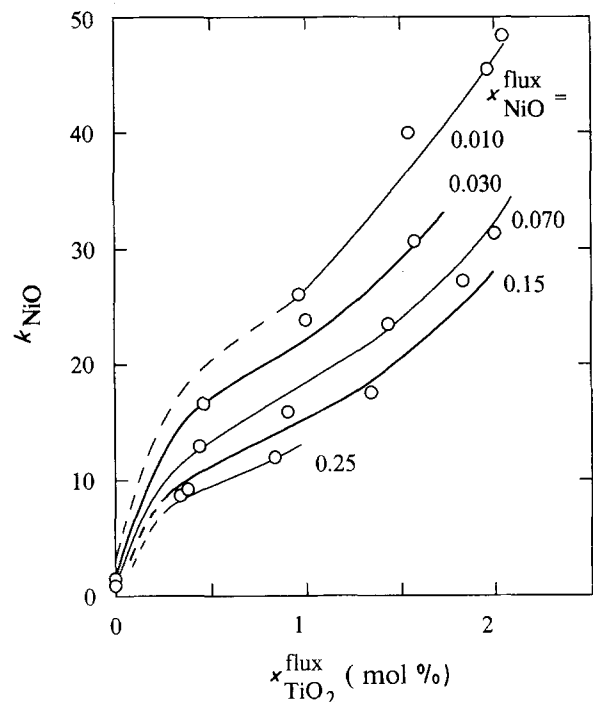
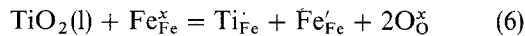


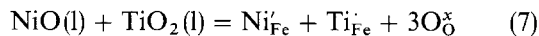
Figure 5 Effect of TiO_2 content in the flux on k_{NiO} as a function of the NiO content in the flux at 1000 °C.

less energy than the substitution accompanied by oxygen ion vacancy formation. As with the result for k_{TiO_2} shown in Fig. 3, the values for k_{NiO} increase with an increased TiO_2 content in the flux at constant NiO content in the flux. It can be seen that the increment of k_{NiO} is greater than that of k_{TiO_2} . The reason for this may be explained as follows: the substitution accompanied by oxygen ion vacancy according to Equation 2 occurs in the experiment of NiO partitioning in $\alpha\text{-Fe}_2\text{O}_3$. On the other hand, the substitution accompanied by the Fe^{2+} formation according to Equation 6 occurs in the experiment of TiO_2 partitioning in $\alpha\text{-Fe}_2\text{O}_3$ [3]. Thus, the increment of k_{NiO} was found to be greater than those for k_{TiO_2} , because the latter substitution requires less energy than the former.

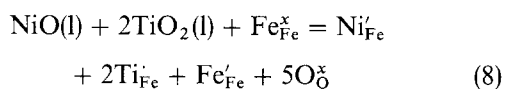


where the symbol Fe'_{Fe} refers to the Fe^{2+} ion.

Roy and Coble [13] studied the coupled substitution of MgO and TiO_2 in Al_2O_3 and proposed the defect equilibrium: $\text{MgTiO}_3(\text{s}) = \text{Mg}'_{\text{Al}} + \text{Ti}_{\text{Al}} + 3\text{O}^{\times}$ in which the electroneutrality is maintained. In the present study, the coupled substitution of TiO_2 and NiO in $\alpha\text{-Fe}_2\text{O}_3$ can be written as



In the $\text{Fe}_2\text{O}_3\text{-FeO-TiO}_2\text{-NiO}$ tetrahedron shown in Fig. 6, the substitution given by Equation 7 corresponds to the solid solution of NiTiO_3 in $\alpha\text{-Fe}_2\text{O}_3$ in the $\text{Fe}_2\text{O}_3\text{-NiTiO}_3$ pseudobinary system. However, as mentioned previously, the formation of Fe^{2+} ions was experimentally confirmed as a result of coupled substitution. Therefore, it appears reasonable that the substitution according to Equation 8 which is the combination of Equations 6 and 7, becomes energetically more favourable.



The reaction given by Equation 8 corresponds to the

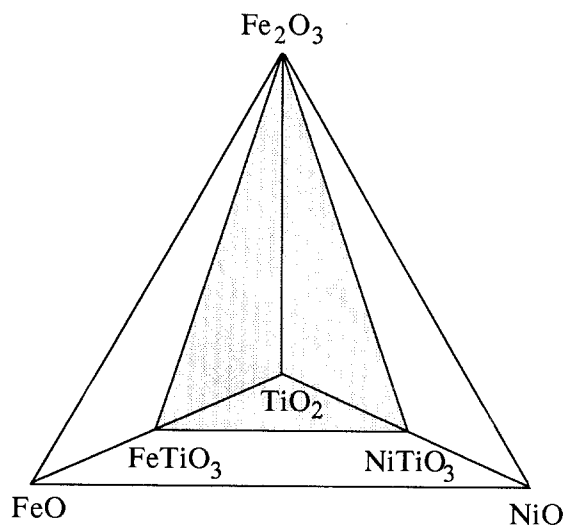


Figure 6 Solid solution surface of Fe_2O_3 and $\text{Ni}_{1-x}\text{Fe}_x\text{TiO}_3$ rhombohedral phases in the $\text{NiO-FeO-Fe}_2\text{O}_3\text{-TiO}_2$ tetrahedron.

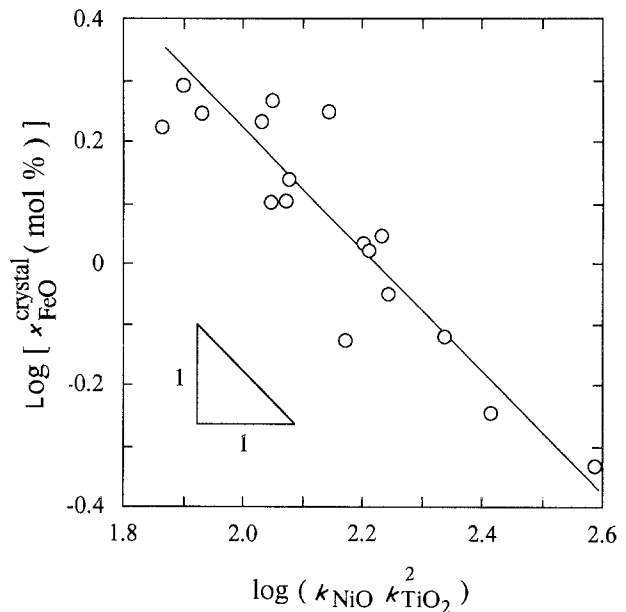


Figure 7 FeO content in the crystal at 1000°C plotted against $k_{\text{NiO}}k_{\text{TiO}_2}^2$ in Equation 9 on logarithmic scales.

solid solution of FeTiO_3 and NiTiO_3 in $\alpha\text{-Fe}_2\text{O}_3$ in the $\text{Fe}_2\text{O}_3\text{-FeTiO}_3\text{-NiTiO}_3$ pseudoternary system shown in Fig. 6, which is predicted from the $\text{Fe}_2\text{O}_3\text{-FeTiO}_3\text{-MgTiO}_3$ pseudoternary system [14].

From Equation 8, we obtain

$$\log(x_{\text{FeO}}^{\times}) = -\log(k_{\text{NiO}}k_{\text{TiO}_2}^2) + C_2 \quad (9)$$

where C_2 is the constant in the present work. The values for x_{FeO}^{\times} are plotted against the term $k_{\text{NiO}}k_{\text{TiO}_2}^2$ on logarithmic scales in Fig. 7, indicating a linearity having a slope of -1 . This suggests that Henry's law is approximately valid in each component in both phases.

4. Conclusions

Distribution experiments of NiO and/or TiO_2 between $\alpha\text{-Fe}_2\text{O}_3$ crystal and $\text{Na}_2\text{O}\cdot 2\text{B}_2\text{O}_3$ melt were carried out. The following conclusions with respect to the substitution mechanism in $\alpha\text{-Fe}_2\text{O}_3$ were derived from the composition dependence of the distribution coefficient.

1. NiO, on dissolving in $\alpha\text{-Fe}_2\text{O}_3$, produces oxygen ion vacancies.

2. The coupled substitution of NiO and TiO_2 in $\alpha\text{-Fe}_2\text{O}_3$ accompanied by the formation of Fe^{2+} ions was explained by the solid solution of the rhombohedral $\text{Ni}_x\text{Fe}_{(1-x)}\text{TiO}_3$ and $\alpha\text{-Fe}_2\text{O}_3$ phases.

References

1. B.-H. PARK and H. SUIITO, *ISIJ Int.* **30** (1990) 426.
2. H. TODOROKI and H. SUIITO, *Scand. J. Metall.* **20** (1991) 211.
3. B.-H. PARK and H. SUIITO, *Can. Met. Quart.*, **31** (1992) 133.
4. H. KELTING and H. WITT, *Z. Phys.* **126** (1949) 697.
5. K. NASSAU, *J. Phys. Chem. Solids* **24** (1963) 154.
6. R. D. SHANNON, *Acta Crystallogr.* **A32** (1976) 752.
7. F. A. KRÖGER and J. K. VINK, in "Solid State Physics",

- edited by F. Seitz and D. Turnbull (Academic Press, New York, 1956) p. 307.
8. O. N. SALMON, *J. Phys. Chem.* **65** (1961) 550.
 9. W. J. HARRISON and B. J. WOOD, *Contrib. Mineral. Petrol.* **72** (1980) 145.
 10. C. WAGNER, *Phys. Chem.* **57** (1953) 738.
 11. W. EITE, in "The Physical Chemistry of the Silicates", 3rd English edn (University of Chicago Press, Chicago, 1954) p. 75.
 12. F. G. SMITH, in "Physical Geochemistry" (Addison-Wesley, MA, 1963) p. 42.
 13. S. K. ROY and R. L. COBLE, *J. Amer. Ceram. Soc.* **51** (1968) 1.
 14. D. H. SPEIDEL, *Amer. J. Sci.* **268** (1970) 341.

*Received 12 August 1991
and accepted 7 May 1992*